

## TEMPORAL VARIATIONS OF DIFFERENT SOLAR ACTIVITY INDICES THROUGH THE SOLAR CYCLES 21-23

Ü. D. Göker<sup>1,2</sup>, J. Singh<sup>3</sup>, F. Nutku<sup>4</sup> and M. Priyal<sup>3</sup>

<sup>1</sup>*Istanbul Gelisim University, Faculty of Economics, Administrative and Social Sciences, Department of Aviation Management, Avclar 34315 Istanbul, Turkey*

E-mail: [udgoker@gelisim.edu.tr](mailto:udgoker@gelisim.edu.tr)

<sup>2</sup>*Physics Department, Boğaziçi University, Bebek 34342, Istanbul, Turkey*

E-mail: [deniz.goker@boun.edu.tr](mailto:deniz.goker@boun.edu.tr)

<sup>3</sup>*Indian Institute of Astrophysics, Koramangala, Bengaluru 560034, India*

E-mail: [jsingh@iiap.res.in](mailto:jsingh@iiap.res.in), [mpriya@iiap.res.in](mailto:mpriya@iiap.res.in)

<sup>4</sup>*Department of Physics, Faculty of Science, Istanbul University, Vezneciler, Istanbul 34134, Turkey*

E-mail: [fnutku@istanbul.edu.tr](mailto:fnutku@istanbul.edu.tr)

(Received: December 9, 2016; Accepted: August 30, 2017)

**SUMMARY:** Here, we compare the sunspot counts and the number of sunspot groups (SGs) with variations of total solar irradiance (TSI), magnetic activity, Ca II K-flux, faculae and plage areas. We applied a time series method for extracting the data over the descending phases of solar activity cycles (SACs) 21, 22 and 23, and the ascending phases 22 and 23. Our results suggest that there is a strong correlation between solar activity indices and the changes in small (A, B, C and H-modified Zurich Classification) and large (D, E and F) SGs. This somewhat unexpected finding suggests that plage regions substantially decreased in spite of the higher number of large SGs in SAC 23 while the Ca II K-flux did not decrease by a large amount nor was it comparable with SAC 22 and relates with C and DEF type SGs. In addition to this, the increase of facular areas which are influenced by large SGs, caused a small percentage decrease in TSI while the decrement of plage areas triggered a higher decrease in the magnetic field flux. Our results thus reveal the potential of such a detailed comparison of the SG analysis with solar activity indices for better understanding and predicting future trends in the SACs.

**Key words. Methods:** data analysis – Sun: activity – Sun: chromosphere – Sun: faculae, plagues – sunspots

### 1. INTRODUCTION

The variability of solar activity indices such as the total solar irradiance (TSI), the F10.7 cm solar radio flux (F10.7) and the E10.7 ultraviolet flux

(E10.7), magnetic activity, sunspot counts (SSCs), number of sunspot groups (SGs), facular area (FA), Ca II K-flux and plage area (PA) is very important in understanding the structure of solar activity cycles (SACs). Detailed statistics for the magnetic flux

will be analyzed by comparing it with time series of other solar activity indices according to the group type and sunspot size. As found by the detailed analysis of Kilcik *et al.* (2011), Lefèvre and Clette (2011), Kilcik *et al.* (2014a, 2014b), there was an important deficit in small groups after the last activity maximum in 2002 while the number of large groups remained largely stable.

For large (D, E and F) SGs, the monthly total number of sunspots was similar in both SACs 22 and 23, while the monthly total sunspot area (SSA) was larger in SAC 22. The average of large SSA was about 25% smaller in SAC 23 than in SAC 22 (Kilcik *et al.* 2011). For small (A and B), medium (C) and decaying (H) SGs, the total number of sunspots was higher in SAC 22 than in SAC 23. In addition to this, the monthly total SSA was larger in SAC 22 than in SAC 23. The average areas of small sunspots were nearly the same in both SACs. In general, the numbers of large SGs reach maxima in the middle of the SAC (phases 0.45-0.5) while the international sunspot numbers (ISSN) and the numbers of small SGs generally peak much earlier (SAC phases 0.29-0.35) (Kilcik *et al.* 2011).

The TSI vary mostly because of changes in the areas of dark sunspots and bright faculae (Chapman, Cookson and Dobias 1997). The number of large and small SGs, and the maximum TSI level for cycle 21 were higher than those for cycle 22 (Kilcik *et al.* 2011). However, de Toma *et al.* (2004) mentioned that the TSI did not change significantly from cycle 22 to cycle 23 despite the decrease in sunspot activity of SAC 23 relative to SAC 22.

The TSI, magnetic activity, SSA and FA show better agreement with the number of large SGs than they do with the small ones (Kilcik *et al.* 2011). However, there are two important solar activity indices such as Ca II K-flux and plage regions which still need to be analyzed and compared with variations of large and small SGs. The intensity calibration of Ca II K-line images, however, is very difficult because of the contributions from the quiet Sun limb darkening curve. In addition to this, observations near the core of the ionized Ca II K-line (393.37 nm) are one of the most effective tools in investigating the morphology and evolution of both plagues and chromospheric magnetic network (Raju and Singh 2014).

In the present paper, TSI, magnetic activity, sunspots/SGs, Ca II K-flux, FA and PA data are examined, and a time series method is done to explain the unexpected variation in solar activity indices in the last SAC (SAC 23). The aim of the paper is comparing the relation between solar activity indices with the number and the different type of sunspots/SGs in SACs 21-23 by applying time series

for the first time. We used the group length to define the class type which is a simple but effective parameter to study spot groups and identify the activity proxies. Thus, we find a relation between different types of SGs and the variation of solar activity indices.

The organization of the paper is as follows. In Section 2, we give the data description and explain the data application technique. In Section 3, we discuss the results and in Section 4, we present our conclusions.

## 2. DATA DESCRIPTION AND APPLICATION TECHNIQUE

### 2.1. Data Description

All SG classification data used here were taken from the National Geographical Data Center<sup>†</sup> and they include various observational parameters of SGs and SSCs for each group recorded during the observed day. The data are collected by the United States Air Force/Mount Wilson Observatory (USAF/MWL). This database also includes measurements from Ramey, Palehau, Learmonth, Rome, Holloman and San Vito Solar Observatories, and others. We used the Rome Astronomical Observatory (ROME), and the Learmonth Solar Observatory (LEAR) data as the principal data source for SAC 21, and SACs 22 and 23 respectively while the gaps were filled with records from one of the other stations listed above, so that a nearly continuous time series was produced. For better comparison, ROME small SGs and ROME large SGs were multiplied by 1.6 and 1.2 to match the LEAR measurements, respectively.

Here, the Zurich classification for cycle 21 and the modified Zurich (McIntosh) classification (McIntosh 1981, 1990) data for cycles 22-23 and the first half of cycle 24 were used (for more details, see Kilcik *et al.* 2011). We followed a technique similar to that given in the work of Kilcik *et al.* (2011) during the selection of classification. The data for TSI and magnetic field (full disk magnetic activity of the Sun) were taken from the SOLAR2000 data<sup>‡</sup> and the Wilcox Solar Observatory<sup>§</sup>, respectively.

The data for faculae and Ca II K-line (393.37 nm) are based on daily synoptic full-disk images obtained by photoelectric photometry of sunspots at the San Fernando Observatory (SFO)<sup>¶</sup>. The plage and Ca II K-flux observations were taken from the Kodaikanal Data (KKL)<sup>||</sup> (Singh *et al.* 2012, Raju and Singh 2014, Priyal *et al.* 2014). However, we preferred using the Ca II K-line images from SFO to compare with the faculae observations from the same observatory.

<sup>†</sup>[ftp://ftp.ngdc.noaa.gov/STP/SOLAR\\_DATA](ftp://ftp.ngdc.noaa.gov/STP/SOLAR_DATA)

<sup>‡</sup><http://www.spacewx.com/solar2000.html>

<sup>§</sup>[http://wso.stanford.edu/meanfld/MF\\_timeseries.txt](http://wso.stanford.edu/meanfld/MF_timeseries.txt)

<sup>¶</sup><http://www.csun.edu/SanFernandoObservatory/>

<sup>||</sup><https://kso.iap.res.in/data>

The detection of PA is very hard and only few observatories have a reliable detection of plage data. The KKL Observatory is one of these research centers, however, there are some problems with obtaining the data. There are gaps in the data due to bad weather conditions; the long gaps are mainly seen in the rainy season (Priyal et al. 2014). In spite of having some gaps depending on the large amount of difference in weather conditions, the KKL Observatory has still got one of the better plage data among the stations.

## 2.2. Data Application Technique

We used daily FA, Ca II K-flux, PA, TSI, magnetic field and monthly averaged SSCs data from 1988/4/25 to 2014/12/29, from 1988/4/25 to 2014/12/29, from 1986/1/6 to 2005/12/28, from 1981/1/1 to 2008/12/31, from 1975/5/16 to 2014/8/3 and from 1982/1/1 to 2014/5/1, respectively. We firstly calculated the absolute value of the magnetic field and then averaged it. Missing days from time versus magnetic field data were dropped. We applied all this data and plotted lines, scatter and bar plots with the use of Python libraries, Pandas (McKinney 2010), NumPy and SciPy (van der Walt et al. 2011) and Matplotlib (Hunter 2007) in Python Notebook environment (Perez and Granger 2007). The application procedure with Python is as follows:

(1) To mitigate the effect of data gaps, we collected the total daily number of SGs and SSCs of a given group type, and then averaged it over the month, thus obtaining a parameter, essentially independent of data gaps. The magnetic field, TSI, FA, Ca II K-flux, PA and the ratio of FA to Ca II K-flux data were grouped for each month in order to be consistent with the monthly averaged SSCs by applying the aggregate function of the arithmetic mean. The merging operation allowed us to compare the data exactly belonging to the same time step.

(2) The cross-correlation technique between SGs and solar activity indices is applied to unsmoothed monthly mean values, and then a simple moving average of time series was calculated. If two data sets were compared over months, data smoothing was done by selecting the window size of the simple moving average as 7 days. This 7-day running mean is clearly seen in the bold continuous curves in all figures throughout the paper.

(3) Bar plots were generated by grouping the time series data into years and averaging the data of each year by its arithmetic mean. Each type of SSC was normalized by dividing it by the sum of all types of SSCs.

(4) After normalization, SSCs were grouped by year, and then averaged for each year. As can be seen from bar plots, the sum of all normalized and averaged SSCs is equal to one for each year. For all histograms, the normalization for each year is given by:

$$\frac{AB}{TSSN} + \frac{C}{TSSN} + \frac{DEF}{TSSN} + \frac{H}{TSSN} = 1 \quad (1)$$

where the total sunspot number (TSSN) was calculated for every month, and then each sunspot number (SSN) divided by TSSN. Here "AB" corresponds to A and B type sunspot groups while D, E and F type sunspot groups are mentioned as "DEF" through the paper to make the identifications easier.

(5) Performing such a normalization allowed us to investigate the relative change of SSCs by type for each year. In order to measure whether there is a linear relation between different time series, Pearson product-moment correlation coefficients were calculated. In general, the Pearson product-moment correlation coefficient of two independent variable sets containing  $n$  items can be calculated by using the following formula:

$$r = r_{xy} = \frac{n \sum x_i y_i - \sum x_i \sum y_i}{\sqrt{n \sum x_i^2 - (\sum x_i)^2} \sqrt{n \sum y_i^2 - (\sum y_i)^2}}, \quad (2)$$

where  $x_1, \dots, x_n$  and  $y_1, \dots, y_n$  are two independent variable sets and  $i$  is the item index.

## 3. RESULTS AND DISCUSSION

### 3.1. Comparison of Sunspot Groups with Magnetic Activity and TSI

To delineate the role of various features of the solar activity indices, we compare the time variations of these parameters with the different type of SG numbers and SSCs. We further investigate the relationship between these parameters during the decreasing phases of SACs 21-23 and increasing phases of SACs 22-23. In Figs. 1(a) and 1(b), we plot the sum of smoothed monthly mean number of SGs (SMMNSGs) and monthly mean number of SSCs (MMNSSCs) for the sunspot classes "AB, C, H" and "DEF" on the right hand side of the  $y$ -axis while the left hand side of the  $y$ -axis corresponds to the scale of magnetic field in the units of  $\mu T$ .

In Figs. 2(a) and 2(b), we plot the sum of SMMNSGs and MMNSSCs for the sunspot classes "AB, C, H" and "DEF" on the right hand side of the  $y$ -axis while the left hand side of the  $y$ -axis corresponds to TSI in the units of  $W/m^2$ . In Fig. 1, the number of AB SGs in the maximum phase of SAC 22 is higher than in SAC 23 and it is the same in the minimum phases (SAC 22 > SAC 21 > SAC 23) and these SGs did not increase even in the beginning of SAC 24. The number of C type SGs is also higher in the maximum of SAC 22 than in SAC 23 and it decreased to zero in the minimum of SAC 23. In DEF groups, there has been no important difference between all cycles and the number of these groups in the first and second maxima are SAC 22  $\gtrsim$  SAC 23 and SAC 22  $\lesssim$  SAC 23, respectively while the minima in SAC 21 showed a similar decrease to the minima in SAC 22. H groups showed similar numbers in the maximum phases of SACs 22 and 23, and no distinct data in the decreasing phase for some observing days. Our results correspond to the work of Kilcik et al. (2014b).

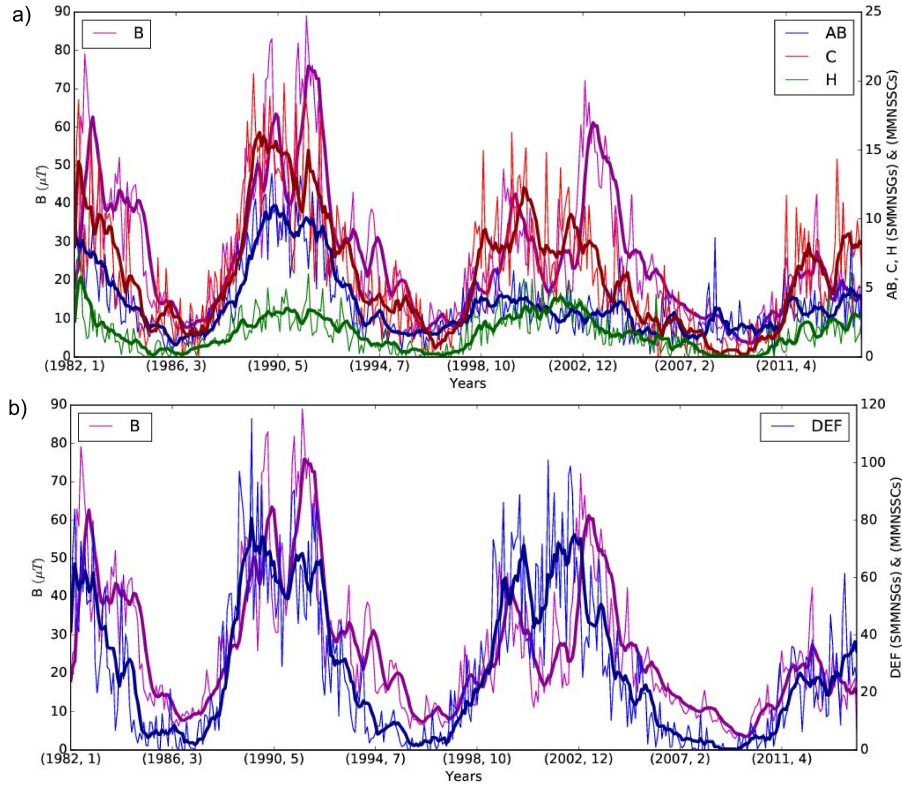


**Fig. 1.** Temporal variations of absolute values of monthly grouped and averaged magnetic field are compared with time series of AB, C, H and the DEF type SGs and SSCs. The thick lines are used for smoothed time series.

The magnetic activity was distinctively lower in SAC 23. Small and large SGs started to rise before the magnetic activity increase occurs in SAC 23 while SGs and magnetic activity change in a synchronized way in SAC 22 as seen in Figs. 1(a) and 1(b). In Fig. 1(a), the second maximum of SAC 22 is seen at the end of 1991 while C type SGs are correlated with the first peak of the magnetic field. However, there is a huge difference in the second peak of the magnetic field in SAC 23 (in the middle of 2003) with C type sunspot groups. In Fig. 1(b), the first (at the end of 1989) and the second (at the end of 1991) peaks of magnetic field are correlated with large SGs. In contrast to this, the magnetic activity is substantially lower in SAC 23 while large SGs are still comparable with SAC 22. Lefèvre and Clette (2011) also found that there was no significant difference in the distributions from D to F groups even in the short lifetime tails and our results prove all these conclusions.

The TSI profile for cycle 23 has a distinct double peak, and the second peak began in the middle of 2001 approximately finishing at the end of 2002, thus coinciding with the peak of the large SG numbers while the double peak in SAC 22 showed comparable increases with large SGs. In SAC 23, large SGs reach their maximum numbers about 2 years later than the small ones as seen in Figs. 1 and 2. This time difference is more effective for the magnetic field than in TSI. Small groups are effective in TSI after

the maxima in SAC 22 (in the beginning of 1990) and in the maxima of SAC 23 (in the year 2000) as seen in Fig. 2(a) and C type SGs are more correlated with TSI profiles both for SACs 22 and 23 than the other small type SGs.

In our results for the variations of magnetic activity and TSI, we found that the intensity of magnetic activity decreased even in the increasing phase of SAC 23 while TSI did not change significantly as compared to previous cycles. Depending on the extended strength of SAC, the average temperature and the magnetic field intensity decrease. Decreasing temperature will cause the decrease of the radiation and intensity. On the other hand, SAC 23 has got its own peculiarities than the other solar cycles and we have referred to this unexpected variation in SAC 23 in our first paper (Göker et al. 2017). From this respect, we approved to apply the connection between magnetic activity, TSI, faculae, Ca II K-flux and plage area, and different type of SSCs/SGs. Particularly, the connection between magnetic activity and small and large SGs was compared for the first time in our work. From this comparison, we found that magnetic activity reached the minimum values with lower small type SGs. Both small and large SGs start to appear before the magnetic field increasing occurs in SAC 23 while SGs and magnetic field are changing in a synchronized way in SAC 22. Small SGs are important for magnetic activity because the

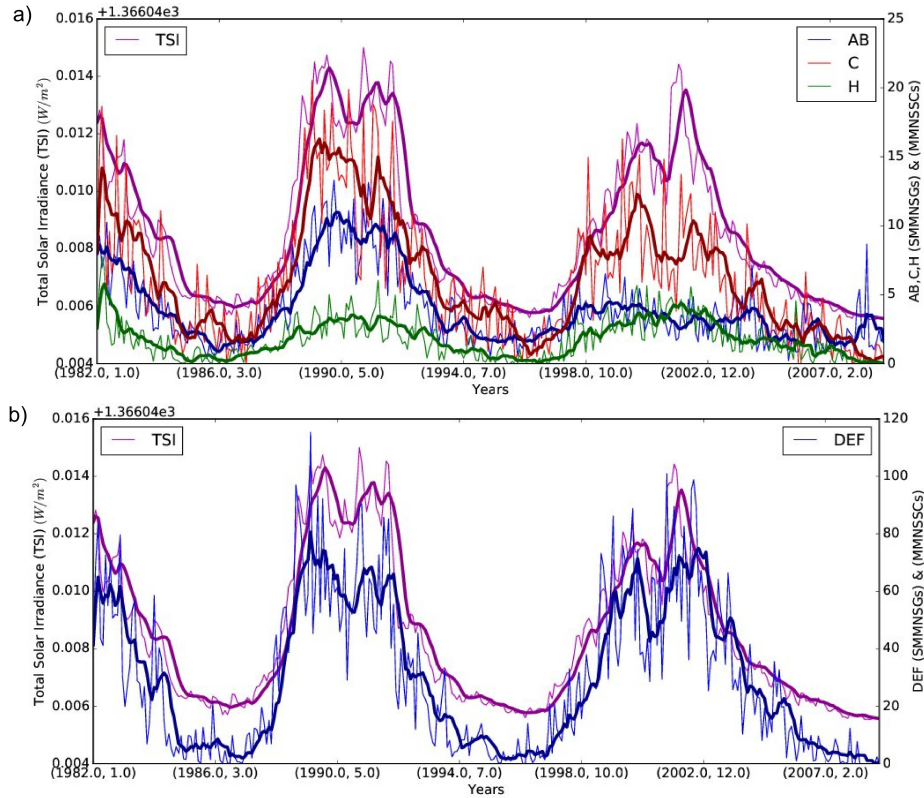


**Fig. 2.** Temporal variations of monthly grouped and averaged TSI are compared with time series of AB, C, H and DEF type SGs and SSCs. The thick lines are used for smoothed time series.

magnetic field is related with small SGs while TSI values are connected with large SGs. The number of small spots show an important decrease from the year 2000 while the number of large spots remained unaffected. This decreasing of small SGs caused the main decrease of magnetic activity rather than the strength of SAC 23. TSI values did not change significantly during the solar cycle 23 because they relate with large SGs and the results of de Toma et al. (2004, 2013) support our results.

We examined the occurrence of spot groups based on their class type in the modified Zurich classification which is based on sunspot morphology and group length while Lefèvre and Clette (2011) and de Toma et al. (2004, 2013) separated SGs according to the group type/spot size and group area, respectively. This is a very important difference between our work and the studies of Lefèvre and Clette (2011) and de Toma et al. (2004, 2013). However, all these studies which are made by using different classification techniques for the same data strongly support our results.

### 3.2. Facular Area and Ca II K-flux

In Figs. 3(a) and 3(b), we plot the sum of SMMNSGs and MMNSSCs for the sunspot classes "AB, C, H" and "DEF" corresponding to the values of Ca II K-flux. In Fig. 3(a), the small SGs and Ca II K-flux variations change synchronously in SAC 22

while they moved away from the correlation in SAC 23 (in the year 1999). The Ca II K-flux variation is 30% lower in SAC 23 than in SAC 22. The first peak is not clearly seen for Ca II K-flux in the last solar cycle (in the year 2000) and the second peak starts in the beginning of the year 2003 as seen in Fig. 3(b). FA and Ca II K-flux were separated from synchronization in the beginning of 1999. FA started to increase since the beginning of 1999 until the middle of 2009 and it started to increase again after the year 2010. Our results for SSCs, SG numbers, FA and Ca II K-flux support the analysis of Kilcik et al. (2011), de Toma et al. (2004, 2013) and Chapman et al. (2014).

In Figs. 3(c) and 3(d), the coverage of FA on the solar surface is maximal during the year 1990 in SAC 22 while it is lower for SAC 23 in the year 2001. FA highly correlates with large SGs rather than with small groups in SACs 22 and 23. The peaks of maxima in years 1990-1992 for SAC 22 and 2001-2003 for SAC 23 correlate with the large SGs as well. The area ratio of faculae to Ca II K-flux was 60% in the SAC 22 and 69% in the SAC 23. This is because of the decrease of Ca II K-flux in the last solar cycle (SAC 23). The coverage of FA on the solar surface decreased by only 20% from SAC 22 to SAC 23, however, this decrease was 30% for Ca II K-flux.

As it can be seen in our results, Ca II K-flux is obviously lower in SAC 23 both for small and large SGs, while, the Ca II K-flux variations are compara-

ble with C (essentially) and DEF type SGs. Small SGs (especially AB type groups) correlate with the Ca II K-flux in SAC 22 while they move away from the correlation in SAC 23 (in the year 1999). In the increasing phase of SAC 23, FA starts to increase from 1996 to 2000 because FA correlates with large SGs. On the other hand, the FA ratio decreases with increasing activity levels whereas FA shows an increase in the decreasing phase of SAC 23 because of large SGs did not change significantly. Another conspicuous feature is the separation from synchronization for FA and Ca II K-flux at the beginning of 1999. FA starts to increase since the beginning of 1999 until the middle of 2009 and it starts to increase again after the year 2010. This is because of the connection between "FA and TSI" and "Ca II K-flux and magnetic activity". The decrease of small SGs caused the decrease of magnetic activity and Ca II K-flux in SAC 23 while large SGs remained unchanged. This is a normal result for Ca II K-flux and magnetic activity because Ca II K-flux is associated with the flux of magnetic field. FA started to separate from synchronization depending on large SGs and this relationship also explains the more or less steady TSI variations between SACs 21-23 because FA and TSI are more related with sunspot counts and group numbers.

In Fig. (4), we applied the yearly variations of solar activity indices in one column and all boxes here give the percentage share of these parameters. In Fig. 4(a), the decrease is clear for Ca II K-flux in SAC 23 and in the ascending phase of SAC 24. This histogram shows that, in the descending phase of SAC 22, the Ca II K-flux decreases with the decreasing percentage of SGs as  $C > DEF > AB$  from 1991 to 1995. However, the total number of large SGs are still higher in the increasing phase of SAC 23. The Ca II K-flux is increasing with DEF SGs, however, the highest increase is seen for AB SGs. The yearly percentage of SGs are shown as  $DEF > AB > C$  in the decreasing phase of SAC 23, the Ca II K-flux substantially decreased and still does not rise to the highest levels. From the year 2001 to 2005 the distribution of SGs was  $DEF > C > AB$ , however, AB type SGs started to increase their number from 2006 to 2009 while the percentage of large SGs decreased.

In Fig. 4(b), FA and Ca II K-flux show similar variations in the increasing phase of SAC 22 from the year 1988 to 1990. In the decreasing phase of SAC 22, the FA is higher in the year 1991 but it is still comparable either for Ca II K-flux or the number of large SGs. In the increasing phase of SAC 23, FA started to increase from 1996 to 2000. The total area of faculae was higher even in the decreasing phase of SAC 23 (from the beginning of 2001) as opposed to Ca II K-flux. The average area of Ca II K-flux (and faculae) in the descending phase of SAC 22, increasing phase of SAC 23, decreasing phase of SAC 23, and beginning of the increasing phase of SAC 24 are 37% (63%), 45% (56%), 13% (87%) and 13% (87%), respectively.

The total area of plages decreases both for the descending and ascending phases of SAC 23 as seen in Fig 4(c). The most important decrease was seen

in the descending phase of SAC 23 (SAC 22 (38%)  $\gg$  SAC 23 (25.3%)), however, it was comparable in the ascending phase of SAC 23 (SAC 22 (19.6%)  $\approx$  SAC 23 (17%)). The average of PA was distinctively lower in the descending phase of SAC 23 (SAC 22 (36%)  $\gg$  SAC 23 (20%)) while it was comparable in the ascending phase of SAC 23 (SAC 22 (23.4%)  $\approx$  SAC 23 (20.4%)).

In Fig. 4(d), we plot the grouped ratio of FA to Ca II K-flux on the left hand side of the  $y$ -axis while the right hand side of the  $y$ -axis corresponds to PA, FA and Ca II K-flux for the given years on the  $x$ -axis. The total area ratio of faculae to Ca II K-flux, the *total* area of plages, faculae and Ca II K-flux percentages are given as 31%, 47.44%, 42% and 34.43% and 46%, 31.3%, 43.87% and 53.28% in the descending phases of SAC 22 and SAC 23, respectively.

The *average* values of the area ratio of faculae to Ca II K-flux, the area of plages, faculae and Ca II K-flux percentages are given as 31.8%, 47.40%, 43.66% and 36.78% and 39%, 26%, 38% and 47.46% in the descending phases of SACs 22 and 23, respectively. When we compare the descending phases of SACs 22 and 23, the highest values were found for the average area of plages in SAC 22 and only the average area of faculae was decreased in SAC 23 in contrast to the total area of faculae. In addition to this, when we compare the bar plots of PA with the averaged SSCs, they are mostly related with DEF and C type SGs rather than AB and H class SGs. We must remember one important thing that there were no available plage data for the whole year of 1997.

Bar graphs in Fig. 4 are very important figures in our work because they are an effective way to compare solar activity indices between different sunspots/SGs; they summarize large data set in a visual form; they show how a group of variables changes over time and this visual representation is designed to make it easier to understand the data presented; it may also highlight the specific relevant features of the data; they make it easy to compare the relative size of quantities and they allow the reader to recognize patterns of trends far more easily than looking at data tables.

### 3.3. Plage Regions

In Fig. 5(a), we plot the sum of SMMNSGs and MMNSSCs for the sunspot classes "AB, C, H" and "DEF" on the right hand side of the  $y$ -axis while the left hand side of the  $y$ -axis corresponds to the values of the monthly grouped and averaged PA. In Fig. 5(a), it is clearly seen that DEF SGs start to rise before the PA evolved, however, the other SGs follow the evolution steps of PA. In addition to this, the area covered by plages on the Sun highly decreased after the middle of the year 2002. In the increasing and decreasing phases of SAC 22, the first and second peaks of DEF SGs were seen at the beginning of 1990 and at the beginning of 1992, respectively while the one and only peak was seen for the PA in the middle of 1991. In the descending phase of SAC

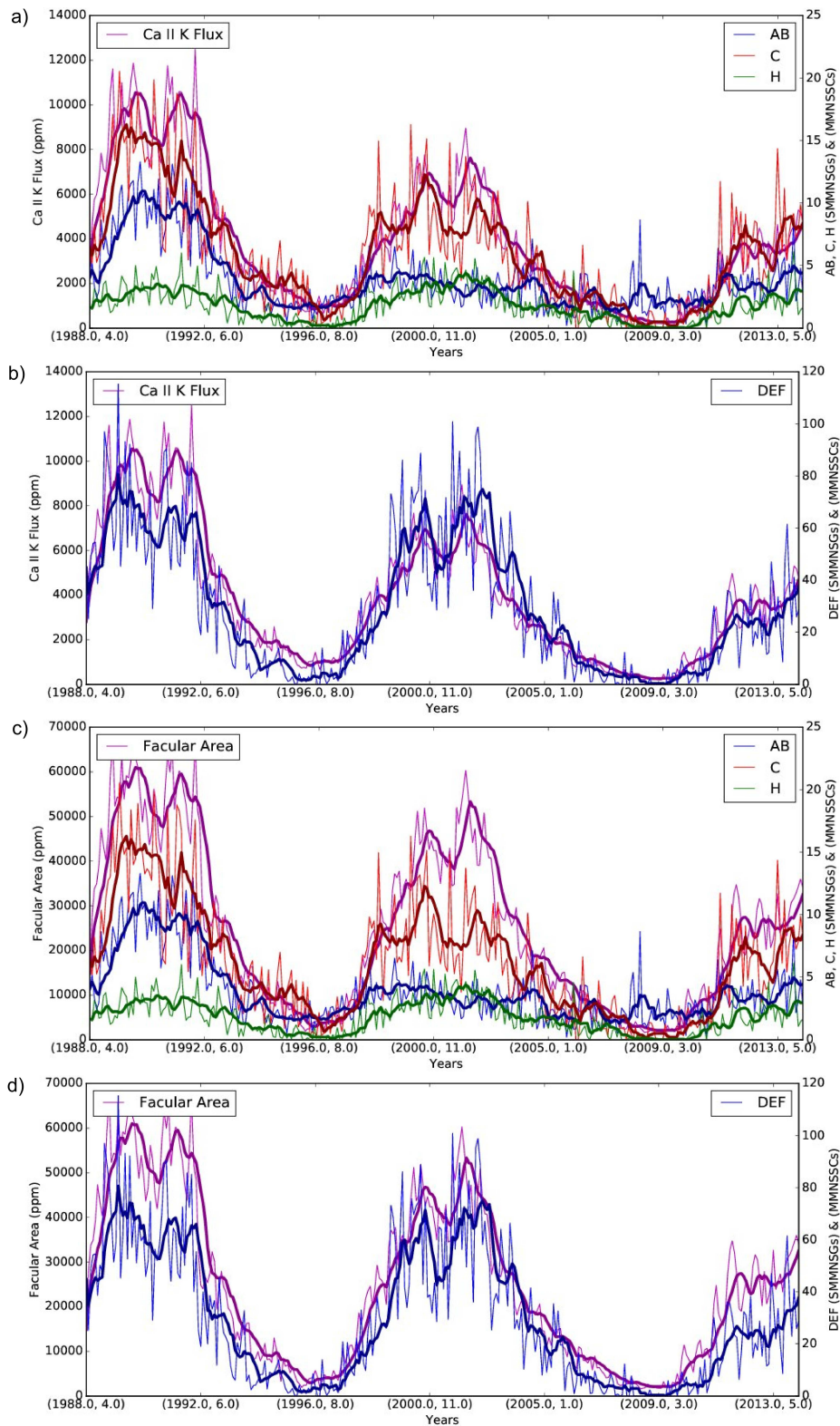


**Fig. 3.** Temporal variations of monthly grouped and averaged Ca II K-flux and FA are compared with time series of AB, C, H and DEF type SGs and SSCs. The thick lines are used for smoothed time series.

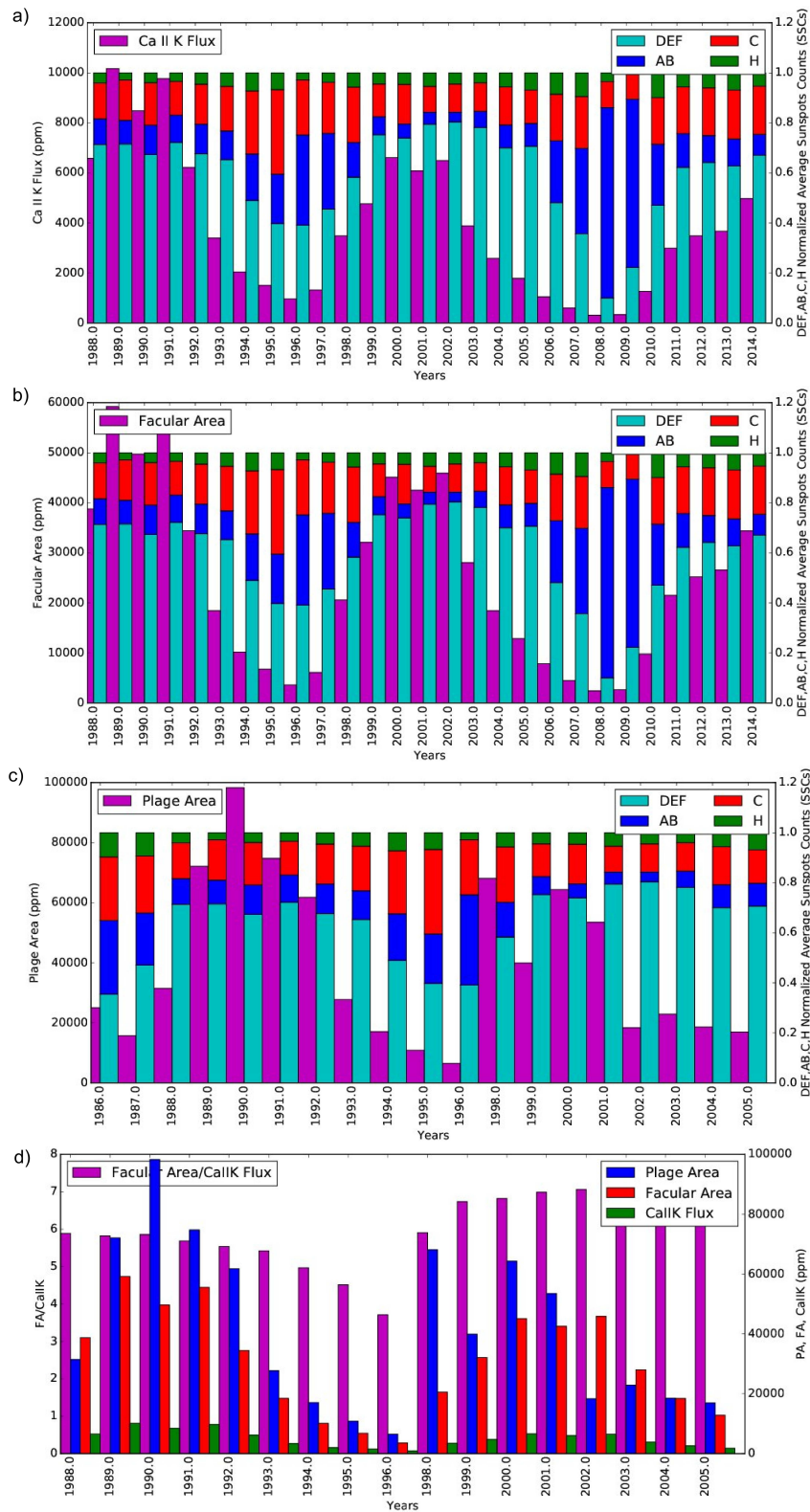


**Fig. 4.** Comparison of Ca II K-flux, FA and PA with normalized average SSCs in time scale of year is given in the first three bar plots while comparison of grouped ratio of FA to Ca II K-flux with PA and FA, and Ca II K-flux in time scale of year is given in panel d.



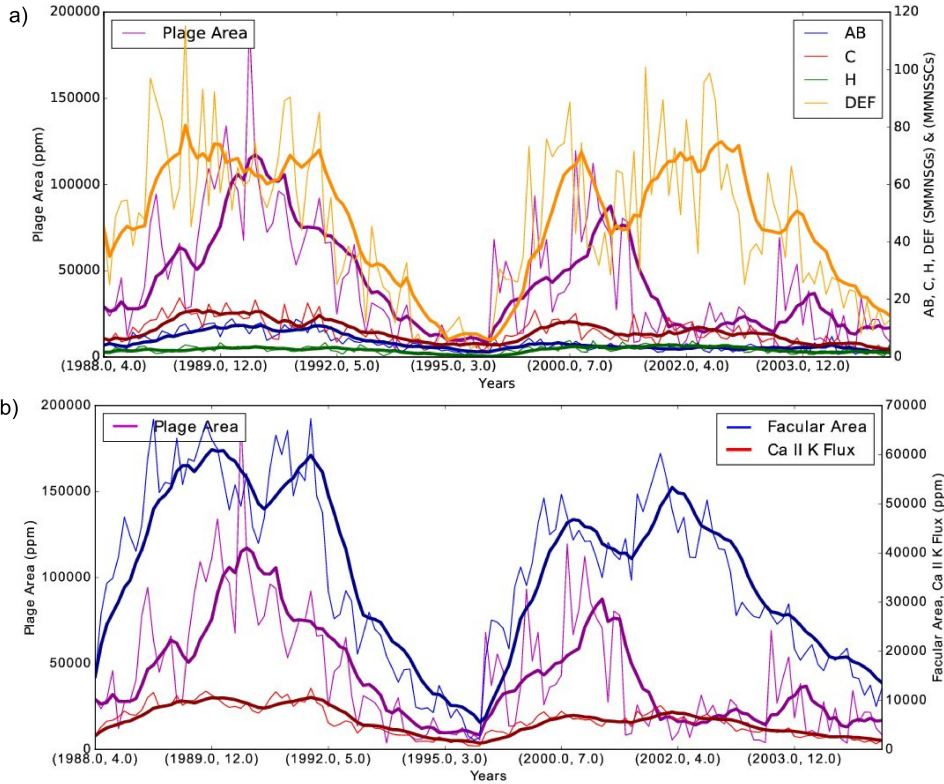


**Fig. 5.** Temporal variations of monthly grouped and averaged PA are compared with time series of AB, C, H and DEF type SGs and SSCs. The thick lines are used for smoothed time series.

**Table 1.** Pearson correlation coefficients ( $r$ ) between Solar activity indices (SI) and AB, C, H and DEF type SGs with their errors.

SI	AB ( $r$ )	C ( $r$ )	H ( $r$ )	DEF ( $r$ )
$ B $	$0.63 \pm 0.12$	$0.63 \pm 0.16$	$0.46 \pm 0.06$	$0.63 \pm 0.84$
TSI	$0.74 \pm 0.57$	$0.84 \pm 0.07$	$0.75 \pm 0.02$	$0.90 \pm 0.84$
FA	$0.71 \pm 0.09$	$0.86 \pm 0.17$	$0.75 \pm 0.05$	$0.90 \pm 0.48$
Ca II K-Flux	$0.76 \pm 0.09$	$0.86 \pm 0.17$	$0.70 \pm 0.05$	$0.87 \pm 0.69$
PA	$0.61 \pm 0.19$	$0.60 \pm 0.19$	$0.27 \pm 0.08$	$0.41 \pm 0.53$

23, the first and second peaks are seen at the end of 2000 and in the middle of 2002, respectively. However the peaks for PA were closer to each other and they were seen approximately at the beginning of 2001. de Toma et al. (2004) showed similar results to our conclusions.

In Fig. 5(b), we plot the monthly grouped and averaged FA and Ca II K-flux on the right hand side of the  $y$ -axis while the left hand side of the  $y$ -axis corresponds to the monthly grouped and averaged PA. From this temporal variation, we found that FA reaches the first peak in the middle of 1990 and second peak at the beginning of 1992 for the increasing phase of SAC 22, however, plage regions show only one peak at the beginning of 1991. In SAC 23, FA shows the first peak at the beginning of 2001 and the second peak in the middle of 2002, however, PA show very close (double) peaks in the middle of 2001.

The total (and the average) area of plagues are decreased both for the decreasing and ascend-

ing phases of SAC 23. PA correlates with C type of SGs more than with the other types. Only DEF SGs start their increase before PA started to appear, and the covered area of plagues on the Sun decrease after the middle of the year 2002. FAs evolve before the evolution of plage regions, and they reach maximum phases earlier than PA. Large SGs are especially effective after the year 2002 and FA is even higher from the beginning of 2001 as opposite to the Ca II K-flux in SAC 23. The covered area of plagues on the Sun decreases after the middle of the year 2002. FA has a strong influence on TSI while magnetic field is strongly related with plage regions. For the Ca II K-flux and plage regions, small SGs, especially C type SGs, are important.

The Pearson correlation coefficient,  $r$ , can take a range of values from +1 to -1. The stronger the association of the two variables, the closer the Pearson correlation coefficient,  $r$ , will be either to +1 or -1 depending on whether the relationship is positive

or negative, respectively. If  $r=0$ , it indicates that there is no association between the two variables. In Table 1, we presented the Pearson correlation coefficients of solar activity indices with different sunspot categories. As seen in Table 1, the Pearson correlation coefficients of TSI, FA and Ca II K-flux highly correlate with C and DEF type SGs while  $|B|$  and PA coefficients have lower correlation values. Especially in PA, these lower values can easily be seen for DEF and H type SGs. From here, we can say that the most important variation in the last SAC was seen for plage regions and this variation also affected the emergence of the magnetic field from the Sun. This unexpected variation in the flux of the magnetic field in SAC 23 was caused by the different physical features of the Sun's itself and the dimension of PA. This variation of large SGs was especially effective in the second maximum peak (after the year 2002) and FA were even higher from the beginning of 2001 while PA decreased after the middle of the year 2002. For this reason, bar graphs in Fig. 4 show these changes more distinctly and they also identify the lower (or higher) values of correlation coefficients in Table 1. This is why we need to add these graphs in our paper. The deviation from a stronger correlation mainly depends two important reason: (1) small amount of data points (e.g. PA data) and (2) unexpected physical conditions during SAC (e.g. SAC 23).

The coefficient of determination,  $r^2$ , is the square of the Pearson correlation coefficient. The coefficient of determination, with respect to correlation, is the proportion of the variance that is shared by both variables. As seen from the coefficient of determination values for TSI, FA and Ca II K-flux activity indices with AB, C and DEF type SGs, the uncertainty is lower (approximately, 20% – 30%) while the uncertainty is increasing for the magnetic field and PA (approximately, 60% – 90%) which is assumed. This increase is caused by the unexpected physical changes in SAC 23 and these uncertain values can only be understood from the inner and/or surface changes from the Sun by using helioseismic models and/or other activity models, respectively.

#### 4. CONCLUSIONS

The anomalous activity from the beginning of SAC 23 can play a significant role in the further development of SAC 24 and in the forecasting of activity parameters for the future cycles. Our current results show the importance of solar activity indices (especially plage regions) to the length of 11yr SAC and their relation between the time distribution of SGs depending on their types. In SAC 23, the surfaces covered by plages on the Sun were smaller and this might have caused the increase of the ratio between facula and plage, and the magnetic flux from the Sun was lower. In spite of a large amount of data being available for plage regions, the reliable detection of plage areas still needs to be put beyond doubt.

In our paper, we compared the relation between solar activity indices with the number and the different type of sunspots/SGs, and found an important connection between them. Namely, large SGs (DEF SGs) follow SACs well-ordered than the small ones, and C and AB type SGs follow this coherence in the second and third orders. This is the key innovation from the previous studies brought by our approach. De Toma et al. (2013) concluded that the total SSA was about 27% lower during the maximum phase of SAC 23 than during the maximum phase of SAC 22, and a similar decrease was also seen in FA and magnetic flux but not in TSI. We found a similar decrease for magnetic flux and total SSA but not in FA and TSI. In SAC 23, large SGs reached their maximum numbers about 2 years later than the small SGs and this difference is more distinctive for the magnetic field than TSI because the magnetic field relates with small SGs and plage regions while large SGs are more sensitive to TSI. In the same way, FAs which connect with TSI are evaluated before the evolution of plage regions, so they would reach the maximum phase before PAs. In this respect, we found a linear relation between large (DEF type) SGs and FA, and a nonlinear relation between DEF SGs and PA. Ca II K-flux and PA variations are comparable with C and DEF type SGs. Kilcik et al. (2011) and de Toma et al. (2014) showed similar connection to our results between TSI, large SGs and bright faculae associated with them for SACs 22 and 23.

The main difference between our discussion of spot groups and the discussion in the work of de Toma et al. (2014) is that they divided the groups into five categories based on their area while we separated groups into only two categories according to their morphology as given by Kilcik et al. (2011). We think the group length used to define the class type is a simple but effective parameter to study spot groups and identify the activity proxies. Chapman et al. (2014) also indicated the importance of the year 1999 with the declining of magnetic activity and the increasing of facular-to-spot-area ratio as it is given in our results and they concluded that the apparent decline in field strength of sunspots is due to a changing distribution of sunspot sizes over time. De Toma et al. (2004) also found lower values for sunspot and facular areas for SAC 23, by about 37% and 46% than SAC 22, respectively. We found a similar lower value for the total area ratio of faculae to Ca II K-flux from our results, but in spite of this, the lower sunspot area value is found only for small SGs (mainly AB type SGs). We also found that FA and Ca II K-flux were separated from synchronization at the beginning of 1999 and FA started to increase.

The results for PA include the most important part in our discussion because obtaining the PA data is not easy and the results obtained for the PA data will complete a big puzzle between the solar activity indices. The most important decrease for the total and the average area of plages was seen in the decreasing phase of SAC 23. From our results, we can say that plage regions and the emergence of the magnetic flux from the Sun have shown the most distinctive variations between SACs 21-23 than the other solar activity indices.

*Acknowledgements* – The authors would like to thank the members of the National Geographical Data Center (NGDC) and World Data Center (WDC) for making USAF\_MWL (mainly Rome) and Learmonth proxies accessible for obtaining and further processing; The Solar Irradiance Platform (SOLAR2000) historical irradiances are provided courtesy of W. Kent Tobiska and Space Environment Technologies (SOLAR2000, the Research Grade empirical solar irradiance model is made available, at no charge, to the science and engineering research community); Wilcox Solar Observatory data used in this study was obtained via the web site <http://wso.stanford.edu> courtesy of J.T. Hoeksema for magnetic field data and the Wilcox Solar Observatory is currently supported by NASA; and the newest data of Stanford Observatory (SFO), California State University, Northridge is used courtesy of Dr. Angela M. Cookson (special contact). The new Sunspot Number data used in this article are produced and distributed by the World Data Center SILSO hosted the Royal Observatory of Belgium, in Brussels. We thank the Director of the WDC-SILSO, Prof. Dr. Frédéric Clette, for providing us with useful guidance and advice for the preparation of this article, and also to Boğaziçi University (Scientific Research Project No: 8563) and The Scientific and Technological Research council of Turkey (TÜBİTAK) for their financial support.

The authors would also like to thank anonymous referee for very useful comments and guidance that improved the presentation of the paper.

## REFERENCES

- Chapman, G. A., Cookson, A. M. and Dobias, J. J.: 1997, *Astrophys. J.*, **482**, 541.
- Chapman, G. A., de Toma, G. and Cookson, A. M.: 2014, *Solar Phys.*, **289**, 3961.
- de Toma, G., White, O. R., Chapman, G. A., Walton, S. R., Preminger, D. G. and Cookson, A. M.: 2004, *Astrophys. J.*, **609**, 1140.
- de Toma, G., Chapman, G. A., Preminger, D.G. and Cookson, A. M.: 2013, *Astrophys. J.*, **770**, 89.
- Göker, Ü. D., Gigolashvili, M. Sh. and Kapanadze, N.: 2017, *Serb. Astron. J.*, **194**, 71.
- Hunter, J. D.: 2007, *Comput. Sci. Eng.*, **9**, 90.
- Kilcik, A., Yurchyshyn, V. B., Abramenko, V., Goode, P. R., Özgüç, A., Rozelot, J.P. and Cao, W.: 2011, *Astrophys. J.*, **731**, 30.
- Kilcik, A., Özgüç, A., Yurchyshyn, V. B. and Rozelot, J.P.: 2014a, *Solar Phys.*, **289**, 4365.
- Kilcik, A., Yurchyshyn, V. B., Özgüç, A. and Rozelot, J.P.: 2014b, *Astrophys. J. Lett.*, **794**, L2.
- Lefèvre, V. and Clette, V.: 2011, *Astron. Astrophys. Lett.*, **536**, L11.
- Mc Intosh, P. S.: 1981, in *The Physics of Sunspots*, ed. L.E. Cram and J. H. Thomas, Sunspot, NM: Sacramento Peak National Solar Observatory, 7.
- Mc Intosh, P. S.: 1990, *Solar Phys.*, **125**, 251.
- Mc Kinney, W.: 2010, *Data Structures for Statistical Computing in Python*, Proc. 9th Python Sci. Conf., 1697900, p. 51.
- Perez, F. and Granger, B. E.: 2007, *Comput. Sci. Eng.*, **9**, 21.
- Priyal, M., Singh, J., Ravindra, B., Priya, T. G. and Amarewari, K.: 2014, *Solar Phys.*, **289**, 137.
- Raju, K. P. and Singh, J.: 2014, *Res. Astron. Astrophys.*, **14**, 229.
- Singh, J., Belur, R., Raju, S., Pichaimani, K., Priyal, M., Gopalan Priya, T. and Kotikalapudi, A.: 2012, *Res. Astron. Astrophys.*, **12**, 201.
- van der Walt, S., Colbert, S. C. and Varoquaux, G.: 2011, *Comput. Sci. Eng.*, **13**, 22.

## ВРЕМЕНСКА ВАРИЈАЦИЈА РАЗЛИЧИТИХ ИНДЕКСА СУНЧЕВЕ АКТИВНОСТИ

Ü. D. Göker<sup>1,2</sup>, J. Singh<sup>3</sup>, F. Nutku<sup>4</sup> and M. Priyal<sup>3</sup>

<sup>1</sup>*Istanbul Gelişim University, Faculty of Economics, Administrative and Social Sciences, Department of Aviation Management, Avcılar 34315 Istanbul, Turkey*

E-mail: [udgoker@gelisim.edu.tr](mailto:udgoker@gelisim.edu.tr)

<sup>2</sup>*Physics Department, Boğaziçi University, Bebek 34342, Istanbul, Turkey*

E-mail: [deniz.goker@boun.edu.tr](mailto:deniz.goker@boun.edu.tr)

<sup>3</sup>*Indian Institute of Astrophysics, Koramangala, Bengaluru 560034, India*

E-mail: [jsingh@iiap.res.in](mailto:jsingh@iiap.res.in), [mpriya@iiap.res.in](mailto:mpriya@iiap.res.in)

<sup>4</sup>*Department of Physics, Faculty of Science, Istanbul University, Vezneciler, Istanbul 34134, Turkey*

E-mail: [fnutku@istanbul.edu.tr](mailto:fnutku@istanbul.edu.tr)

УДК 523.982.6

*Стручни чланак*

Овде поредимо број Сунчевих пега и број група Сунчевих пега (SG) са варијацијом тоталне инсолације (TSI), магнетне активности, CaII K-флуksа, факулама и плажама. Применили смо методу временских серија за добијање података током опадајућих фаза циклуса Сунчеве активности (SAC) 21, 22 и 23, као и током фаза пораста циклуса 22 и 23. Наши резултати указују да постоји јака корелација између индекса Сунчеве активности и промене у малим (A, B, C и H-модификованим групама по Пиришкој класификацији) и великим (D, E и F) SG. Овај донекле неочеки-

вани резултат указује да су плаже значајно мање упркос већем броју великих SG у SAC 23, док се Ca II K-флуks није смањило за велику вредност, нити је био упоредив са SAC 22, и одговара C и DEF типовима SG. Поред тога, пораст факула под утицајем великих SG узроковао је мали процентуални пад у TSI, док је смањење плажа проузроковало веће смањење флуksа магнетног поља. Наши резултати стога показују да је могуће такво детаљно поређење анализе SG са индексима Сунчеве активности зарад бољег разумевања и предвиђања будућих трендова у SAC.